Hindawi Publishing Corporation
International Journal of Photoenergy
Volume 2014, Article ID 210751, 10 pages
http://dx.doi.org/10.1155/2014/210751

Research Article

Oxidation of 4-Chlorophenol by Mesoporous Titania: Effect of Surface Morphological Characteristics

Osmín Avilés-García,[1] Jaime Espino-Valencia,[1] Rubí Romero,[2] José Luis Rico-Cerda,[1] and Reyna Natividad[2]

[1] *Facultad de Ingeniería Química, Universidad Michoacana de San Nicolás de Hidalgo, Edifico V1, Ciudad Universitaria, 58060 Morelia, MICH, Mexico*
[2] *Centro Conjunto de Investigación en Química Sustentable, UAEMéx-UNAM, Km 14.5 Carretera Toluca-Atlacomulco, San Cayetano, Piedras Blancas, Toluca, MEX, Mexico*

Correspondence should be addressed to Jaime Espino-Valencia; jespinova@yahoo.com.mx and Reyna Natividad; reynanr@gmail.com

Received 28 February 2014; Accepted 1 April 2014; Published 27 April 2014

Academic Editor: Wei Xiao

Mesoporous nanocrystalline anatase was prepared via EISA employing CTAB as structure directing agent. The drying rate was used as a key synthesis parameter to increase the average pore diameter. The resultant mesoporous crystalline phases exhibited specific surface areas between 55 and 150 $m^2\ g^{-1}$, average unimodal pore sizes of about 3.4 to 5.6 nm, and average crystallite size of around 7 to 13 nm. These mesophases were used as photocatalysts for the degradation of 4-chlorophenol (4CP) with UV light. Under the studied conditions, the mesoporous anatase degraded 100% 4CP. This was twice faster than Degussa P-25. 57% reduction of chemical oxygen demand (COD) value was achieved.

1. Introduction

TiO_2 is well known as the photocatalyst by excellence. It has been successfully applied to degrade and mineralize a vast amount of hazardous compounds in both air and water [1–5], under mild reaction conditions (low temperature and atmospheric pressure). Within photocatalysis area, it has been widely accepted that the catalyst feature determining its activity is the crystalline structure. Although this is true, other surface characteristics should not be completely left aside. This work aims to report the effect of surface morphological characteristics on mesoporous nanocrystalline anatase activity. The synthesis of the material was conducted by evaporation induced self-assembly approach (EISA). This method was elected since it is a powerful synthesis method to design technologically relevant and functional oxides in the fiber, particle, and film form at the nanoscale [6–9]. The method relies on using very dilute surfactant initial concentration from which a liquid crystalline mesophase is gradually developed upon solvent evaporation. The slow coassembly between the inorganic network and the liquid crystalline phase leads to the formation of long-range order of well-defined mesostructures. The preparation of mesoporous titania particles by EISA has been studied by independent research groups [10–13]. It is expected that a change in size, shape, and dimensions of the mesopore TiO_2 modifies the accessibility, adsorption, and diffusion of guest molecules within the pore network, thereby achieving further degradation. The photocatalytic activity of the synthesized TiO_2 was tested in the degradation of 4-chlorophenol (4CP).

Chlorinated aromatic compounds are a class of compounds widely used and constitute a particular group of priority pollutants. This is mainly due to their numerous origins (pesticide, paint, solvent, pharmaceutics, wood preserving chemicals, coke oven, and pulp industries) [14, 15] and toxic effects. They can be found in ground water, wastewater, and soil. In particular, chlorophenols (CPs) pose serious ecological problems as environmental pollutants due to their

high toxicity, recalcitrance, bioaccumulation, strong odor emission and persistence in environment, and suspected carcinogen and mutagen effect on the living [16, 17]. The photocatalytic degradation of chlorinated phenols in TiO_2 suspensions has been studied by many investigators [18–24]. The results show that phenolic compounds are degraded completely to CO_2 and H_2O through a mechanism involving hydroxylation of the aromatic ring. In particular, 4-chlorophenol (4CP) has been accepted as the standard pollutant for heterogeneous photocatalysis. The photocatalytic degradation of 4CP has been the topic of many investigations [25–29], and the kinetics of the photocatalytic degradation has been extensively studied [30–36]. Despite this vast literature, it still remains unclear whether there is an interaction or not between 4CP degradation and surface morphological characteristics of the employed photocatalyst. Therefore, it is relevant to conduct this study not only in the context of 4CP degradation but also in general within photocatalysis area.

2. Experimental

2.1. Materials and Synthesis. Titanium (IV) ethoxide ($C_8H_{20}O_4Ti$, 80% Aldrich) and titanium (IV) butoxide ($C_{16}H_{36}O_4Ti$, 97% Aldrich) were used as precursors. Hexadecyltrimethylammonium bromide, denoted as CTAB ($C_{19}H_{42}NBr$, 99% Sigma), was used as the structure directing agent (SDA). Ethanol (99.6%, Sigma-Aldrich) was used as organic solvent. Nitric acid (65.2%, Sigma-Aldrich) was used as catalyst.

The synthesis was performed as follows. An alcoholic solution of the precursor was prepared. This solution was added to the SDA under vigorous stirring, and then nitric acid was added dropwise. The resultant solution was stirred at room temperature for 3 h and then was dried at room temperature. Samples with different drying rates were placed in a rotary evaporator at 100 rpm (Heidolph G3 model) using oil as a heating medium. The synthesized powders were then calcined at 350°C and 400°C. It is worth clarifying that samples calcined at 350°C were first calcined at 300°C for 1 hour and then at 350°C for 4 hours with controlled heating and cooling rate of 1°C min^{-1} to remove the SDA. The same heating rate was used for the samples calcined at 400°C. The molar ratio of the as prepared samples was 1 precursor : 3.55 HNO_3 : 0.018 CTAB : 18.71 ethanol.

2.2. Characterization. Mesoporous titania samples were analyzed by X-ray diffraction (XRD) in a Bruker D8 Advanced diffractometer with Cu Kα radiation and a LynxEYE detector. BET surface areas and N_2 adsorption-desorption isotherms were obtained in an Autosorb-1 Quantachrome. Before measurements, samples were degassed at 250°C for 2 h. TEM images were taken with a JEOL-2100 200 kV LaB6 filament. The morphology and particle size of the mesophases were inspected with a SEM JEOL JSM-6510LV.

2.3. Heterogeneous Photocatalytic Oxidation of 4CP. Photocatalytic degradation studies of 4CP were performed in a batch photoreactor of cylindrical shape (see Figure 1). The photoreactor was provided with ports in the lower and upper section for the inlet and outlet of gases and for sampling. Mesoporous titania samples were placed in the glass reactor under continuous stirring (1000 rpm). The total reaction volume was 30 mL. Tests were performed using 0.8 g L^{-1} of mesoporous titania at an initial pH value of 2 and 4CP initial concentration $[4CP]_0$ was 0.233 mmol L^{-1}. The pH adjustment was made by using 0.003 M HCl solution. The temperature throughout the experiment was kept constant at 20°C. The UV lamp was placed at the center of the reactor as the source of UV radiation (254 nm at 0.786 watts cm^{-2}). Oxygen flow of 50 mL min^{-1} was constantly fed at the bottom of the reactor and an oxygen trap was used to increase its residence time. Aliquots samples (0.5 mL) were withdrawn from the system every 30 minutes during 3 hours. Catalyst was removed before analysis.

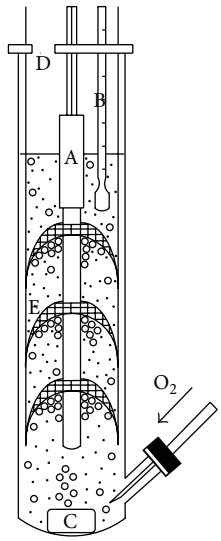

Figure 1: Experimental set-up. (A) UV lamp, (B) thermometer, (C) magnetic stirrer, (D) gas outlet and sampling, and (E) oxygen trap.

At all experiments, the concentration of 4CP (C_{4CP}) was determined using UV/Vis spectroscopy in a Perkin-Elmer Model Lambda 25 UV/Vis spectrophotometer with a wavelength range of 200–360 nm, where the characteristic absorption peak for 4-chlorophenol is located at 280 nm. A calibration curve was constructed from 0 to 0.311 mmol L^{-1}. A determination coefficient of $r^2 = 0.9994$ and a slope of $\varepsilon b = 0.0119$ were obtained. The experiments were repeated three times to verify results reliability.

The chemical oxygen demand (COD) value was analyzed with a Hach UV/Vis Model DR-5000 spectrophotometer in order to determine the degree of oxidation of the 4-chlorophenol after the photocatalytic tests.

3. Results and Discussion

3.1. Catalysts Characterization. The textural properties of the synthesized mesoporous titania with different type of drying are summarized in Table 1. The mesoporous samples that were dried at room temperature exhibited specific

Table 1: Specific surface area, average pore size, and average crystallite size of mesoporous titania samples with different type of drying.

Drying	Precursor	Sample ID	Calcination (°C)	Specific surface area (m^2/g)	Average pore size (nm)	Average crystallite size (nm)
Room temperature	Titanium ethoxide	AE3	350	117	3.4	7
		AE4	400	71	3.4	11
	Titanium butoxide	AB3	350	99	3.4	9
		AB4	400	55	3.4	13
Rotary evaporator	Titanium ethoxide	RE3	350	115	3.8	9
		RE4	400	87	4.3	11
	Titanium butoxide	RB3	350	145	4.3	8
		RB4	400	108	4.9	10

Table 2: Specific surface area, average pore size, and average crystallite size of mesoporous titania samples with different drying rate in rotary evaporator.

Drying rate	Calcination (°C)	Sample ID	Specific surface area (m^2/g)	Average pore size (nm)	Average crystallite size (nm)
Fast	350	FR3	150	3.8	8
	400	FR4	103	4.3	10
Medium	350	MR3 (RB3)	145	4.3	8
	400	MR4 (RB4)	108	4.9	10
Slow	350	SR3	147	4.9	8
	400	SR4	108	5.6	10

surface areas of around 117 $m^2\,g^{-1}$ and average pore size of approximately 3.4 nm. Furthermore, it was observed that the pore diameter remains constant and independent of the calcination temperature. However, the calcination conducted at 400°C decreases the specific surface area. Mesoporous samples dried in rotary evaporator exhibited specific surface areas of approximately 145 $m^2\,g^{-1}$ and average pore size of around 4.9 nm. Furthermore, it was observed that the calcination temperature modifies both the specific surface area and average pore diameter. For this type of drying, the best textural properties were obtained using titanium butoxide as precursor. The reactivity of the precursor determines the rates of hydrolysis and condensation to generate the final inorganic oxide structure. Also, the time used in these processes must be sufficient to allow proper interaction between the SDA and the inorganic precursor and generate assembly and organization in regular structures that finally will lead to an ordered mesoporous structure. For this reason, the titanium butoxide as precursor provides a more controlled reactivity and easy handling, thus allowing control of the hydrolysis and condensation reactions, as well as the dimensions of the pores directly related to the size of the alkoxy groups [37, 38].

The textural properties of the mesoporous titania phases synthesized with titanium butoxide as precursor and different drying rate in a rotary evaporator are summarized in Table 2. Specific surface areas and average pore size of samples were around 150 $m^2\,g^{-1}$ and 5.6 nm, respectively. When the drying rate became slower (at the same calcination temperature), the average pore diameter is observed to increase. Furthermore, the calcination temperature is found to be the only variable that modifies the specific surface area for these samples. Thus, the influence of the evaporation rate of volatile entities is a key parameter that determines the final mesostructure. The slow and gradual evaporation of the solvent promotes progressive increase in the concentration of the SDA by obtaining the critical micellar concentration (CMC), surfactant micelle formation, and their self-assembly with inorganic species at a specific time where the network is flexible enough leads to greater micellar arrangement [39].

The average crystallite size for all samples was estimated using the Scherrer equation and the FWHM of anatase (1 0 1) reflection. Crystal growth increases with a calcination temperature of 400°C for all samples. With increasing calcination temperature, the peak intensity of anatase increases (Figure 2), and the width of the (101) peak becomes narrower due to the growth of anatase crystallites. The pore diameter increase is caused by shrinkage of the mesoporous framework at higher temperatures [40].

The XRD patterns of all the mesophases exhibited only the characteristic reflections of anatase at approximately 2θ of 25°, 38°, 48°, 54°, 55°, and 63°. These correspond to the (1 0 1), (0 0 4), (2 0 0), (1 0 5), (2 1 1), and (2 0 4) planes, respectively, of tetragonal titania [13, 41] as shown in Figure 2.

Nitrogen adsorption-desorption isotherms and the Barrett-Joyner-Halenda (BJH) pore size distribution of synthesized samples are shown in Figure 3. All of these samples show a IV type isotherm with H_2 hysteresis loop, which is representative of mesoporous materials [42].

The TEM images of the mesoporous anatase samples AB4 (dried at room temperature) and SR4 (slow drying rate in rotary evaporator) are shown in Figure 4. For these samples,

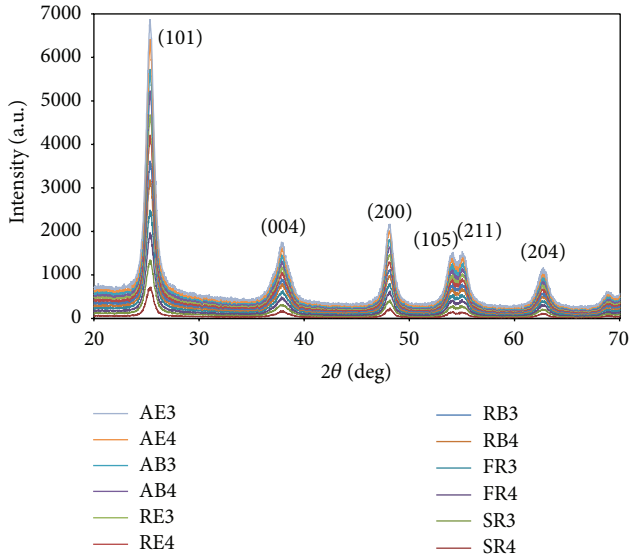

Figure 2: XRD patterns of the prepared mesoporous anatase samples.

Table 3: Initial reaction rates and removal of 4CP with the titania samples and Degussa P-25.

Sample ID	4CP degradation rate $-r_{4CF0} \times 10^8$ (mol/g seg)	Removal of 4CP (%)
AE3	6.30	69
AE4	2.47	62
AB3	8.85	67
AB4	3.93	60
RE3	3.92	75
RE4	7.00	80
RB3	10.27	86
RB4	4.68	93
FR3	5.94	77
FR4	4.42	82
SR3	10.46	95
SR4	13.54	100
Degussa P-25	6.97	57

the anatase crystals were determined to be approximately 13 and 10 nm in size, respectively. The spacing of 0.35 nm, measured for these two sets of fringes, coincides with 0.352 nm, that is, with the d-spacing of (1 0 1) type planes in the anatase form of titania, and this was confirmed by XRD data (Figure 2).

Figure 5 shows SEM images of the mesoporous anatase samples SR4 and AB4. The synthesized mesophase SR4 exhibited clusters of approximately 5–10 μm while the synthesized mesophase AB4 resulted in the formation of larger clusters of approximately 5–14 μm with irregular shapes.

The reference material Degussa P-25 contains anatase and rutile phases in a ratio of about 3 : 1. Anatase and rutile particles separately form their agglomerates and the average sizes of the anatase and rutile elementary particles are 85 and 25 nm, respectively [43]. Furthermore, their specific surface area is 52 $m^2 g^{-1}$ and the average crystallite size is 30 nm [44].

3.2. 4CP Degradation. The mesoporous anatase phases were evaluated in the photodegradation of 4CP. The photoactivity of these samples was compared to that of the reference material Degussa P-25. Figure 6 shows the photocatalytic degradation profiles of 4CP over the mesoporous titania samples and Degussa P-25. All synthesized titania samples showed a higher percentage of degradation than titania Degussa P-25. This may be related to the smaller crystallite size and relatively ordered pore structure of the obtained mesophases. Also, the enhanced photocatalytic activity of the mesoporous titania samples can be partially attributed to the presence of pure anatase phase which is the primary photoactive phase [45].

The mesoporous samples dried at room temperature (Figure 6(a)) and the ones dried in a rotary evaporator (Figure 6(b)) degraded approximately 60–69% and 75–93% of 4CP, respectively, after 180 min. Degussa P-25 degraded only 57% of 4CP after the same time of exposure to UV irradiation. Although mesoporous titania samples dried at room temperature showed the same average pore diameter of 3.4 nm, in Figure 6(a) it is evident that there are differences in the percentages of 4CP degradation due to different specific surface areas. For mesoporous titania samples dried in a rotary evaporator, the highest percentage of degradation (approximately 93%) was obtained with the highest average pore diameter of 4.9 nm (sample RB4), despite not having the largest specific surface area.

The mesoporous titania samples synthesized with different drying rate in a rotary evaporator (Figure 6(c)) degraded approximately 77–100% of 4CP. In Figure 6(c) it is evident that the increase in the percentage of degradation of 4CP is related to the increase in average pore diameters of synthesized samples, since the sample SR4 (average pore diameter of 5.6 nm and specific surface area of 108 $m^2 g^{-1}$) achieves 100% of 4CP degradation in 180 minutes and the sample SR3 achieved only 95% of degradation at the same time, despite having higher specific surface area (147 $m^2 g^{-1}$) and smaller average pore diameter of 4.9 nm. The ordered pore architecture of the mesoporous samples as compared to Degussa P-25 may result in higher diffusion rates of the guest molecules, and therefore the photocatalytic reaction rate increases. The benefits of having an ordered mesopore structure for photocatalytic applications have been demonstrated by independent research groups [46–48].

Table 3 shows the initial rates of degradation of 4CP for all samples synthesized and Degussa P-25. No effect of the average pore diameter was observed on the initial rate of degradation for the samples dried at room temperature. This may be due to several factors such as crystal size, because, when this decreases, the surface density of active sites available for substrate adsorption increases, thus increasing the photocatalytic reaction rate [49, 50].

Figure 7 shows the removal of 4CP by photocatalysis, adsorption, and photolysis using mesoporous titania sample

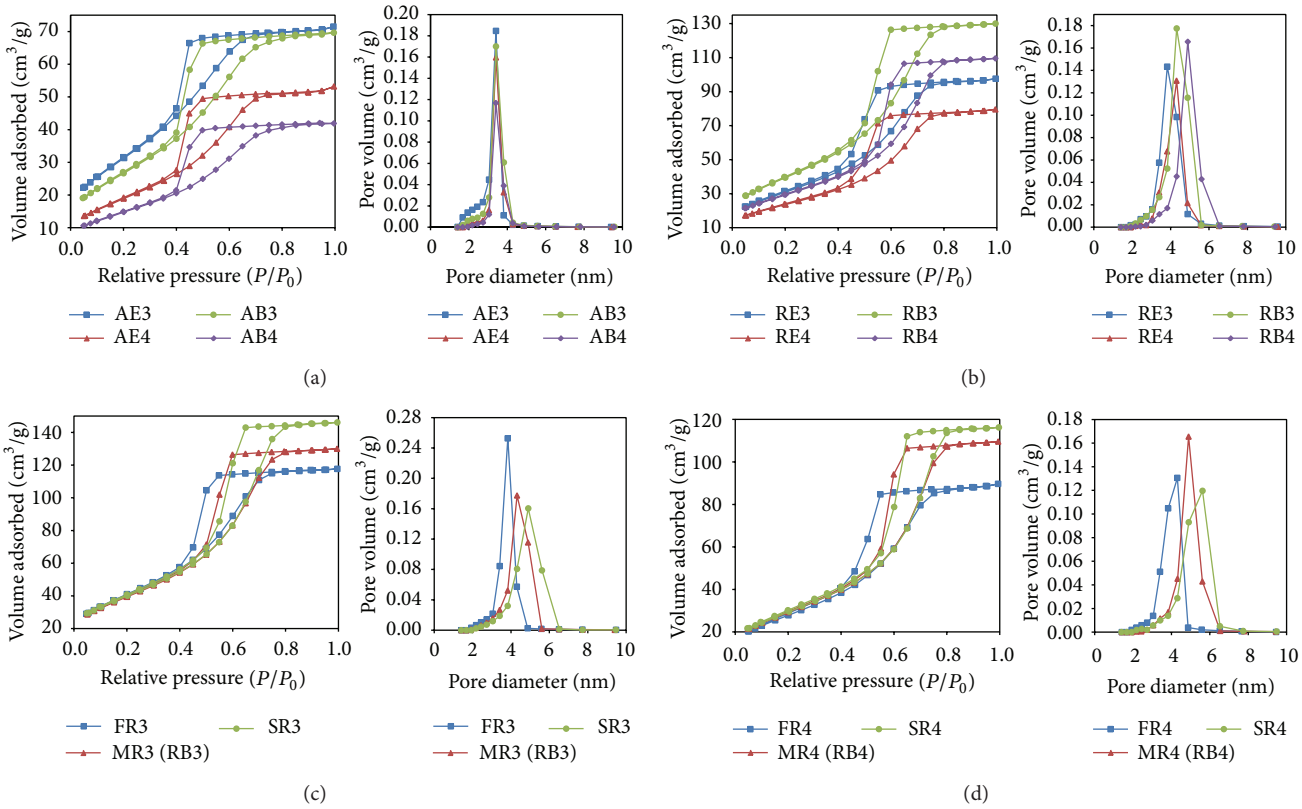

Figure 3: N_2 adsorption-desorption isotherms and pore size distribution of the mesoporous anatase phases dried (a) at room temperature (b) in rotary evaporator (c) with different rate in rotary evaporator and calcined at 350°C (d) with different rate in rotary evaporator calcined at 400°C.

Table 4: Apparent constant, half-life, and linearization coefficient for the Langmuir-Hinshelwood model for 4CP photodegradation.

Sample ID	k_{ap}	$t_{1/2}$ (min)	r^2
AE3	6.60	105.0	0.948
AE4	5.69	121.8	0.968
AB3	5.50	126.0	0.895
AB4	5.46	127.0	0.920
RE3	7.79	89.0	0.996
RE4	8.52	81.3	0.968
RB3	11.02	63.0	0.981
RB4	14.68	47.2	0.997
FR3	8.57	80.9	0.976
FR4	9.53	72.7	0.970
SR3	15.85	43.7	0.987
SR4	27.07	25.6	0.996
Degussa P-25	4.40	157.5	0.864

SR4 since 100% of 4CP degradation was achieved in 180 minutes. The effect of photolysis was studied by carrying out the experiment only in the presence of oxygen and UV light without mesoporous titania. The degradation of 4CP by direct photolysis is negligible, and the increase in concentration is due to an electronic effect that modifies the UV absorbance spectrum and appears as if it was an increase in concentration (Figure 8). This phenomenon has been described as a photoinduction period associated with reactions involving the formation of free radicals [51–53]. Furthermore, the removal of 4CP by adsorption is considered negligible (Figure 7).

The kinetics of photocatalytic reactions of organic compounds are usually adequately described by the Langmuir-Hinshelwood model [29, 51]. It relates the degradation rate

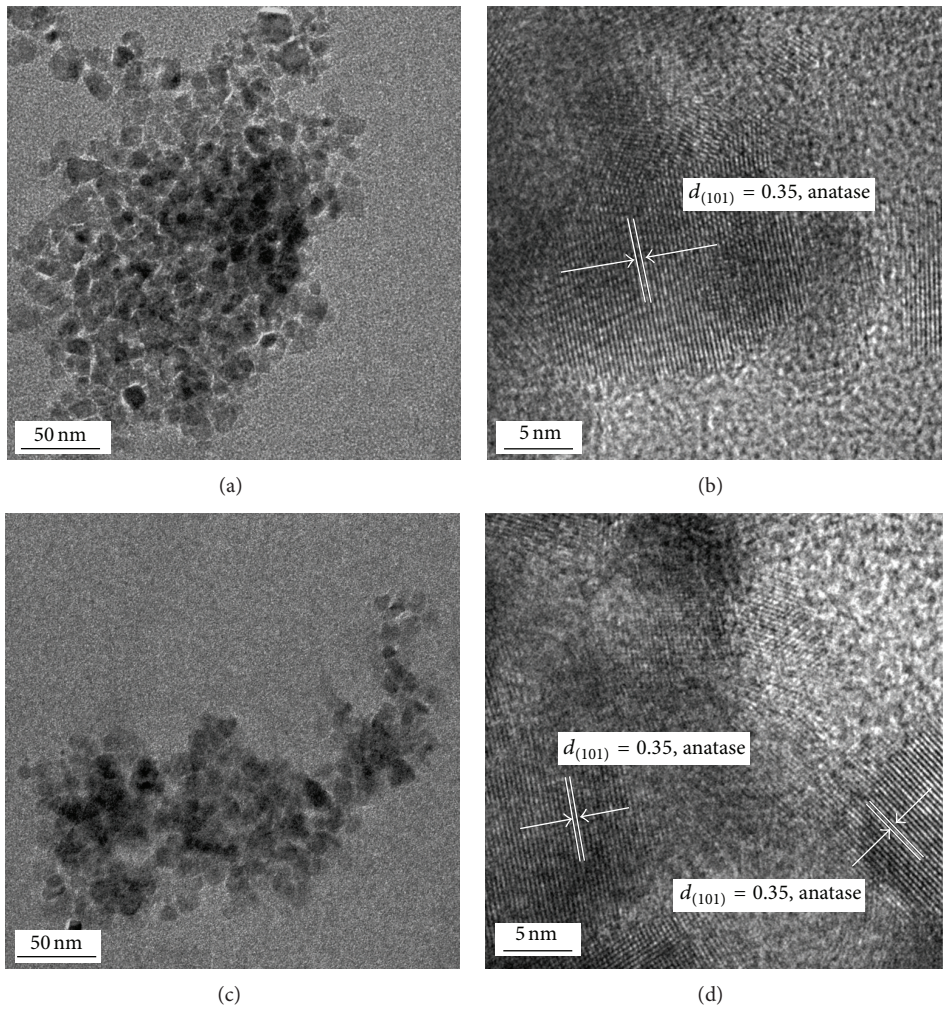

Figure 4: (a) and (c) TEM images of mesoporous nanocrystalline anatase samples AB4 and SR4. (b) A magnified image of (a) and (d) a magnified image of (c) with the d-spacing (1 0 1) of anatase form of titania.

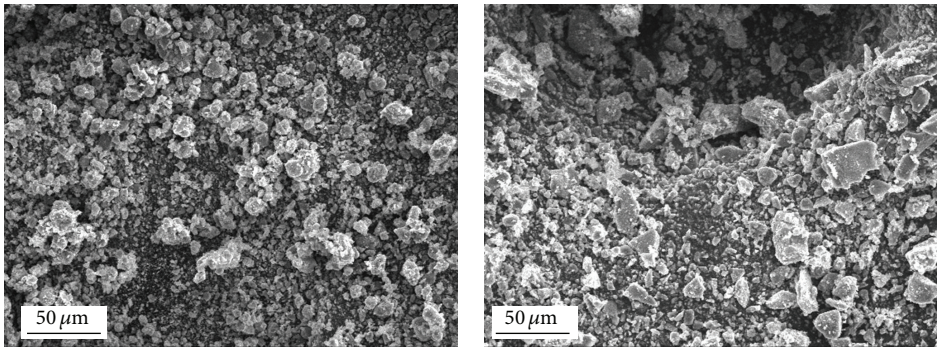

Figure 5: SEM images of the mesoporous anatase phases (a) SR4 (b) AB4.

r and the concentration of organic compound C and is expressed as follows:

$$r = -\frac{dC}{dt} = \frac{k_r K_{ad} C}{1 + K_{ad} C}, \quad (1)$$

where k_r is the intrinsic rate constant and K_{ad} is the adsorption equilibrium constant. If adsorption is weak and concentration of organic compounds is low, the factor $K_{ad}C$ is negligible, and thus (1) can be simplified to the first-order kinetics with an apparent rate constant ($K_{ap} = k_r K_{ad}$),

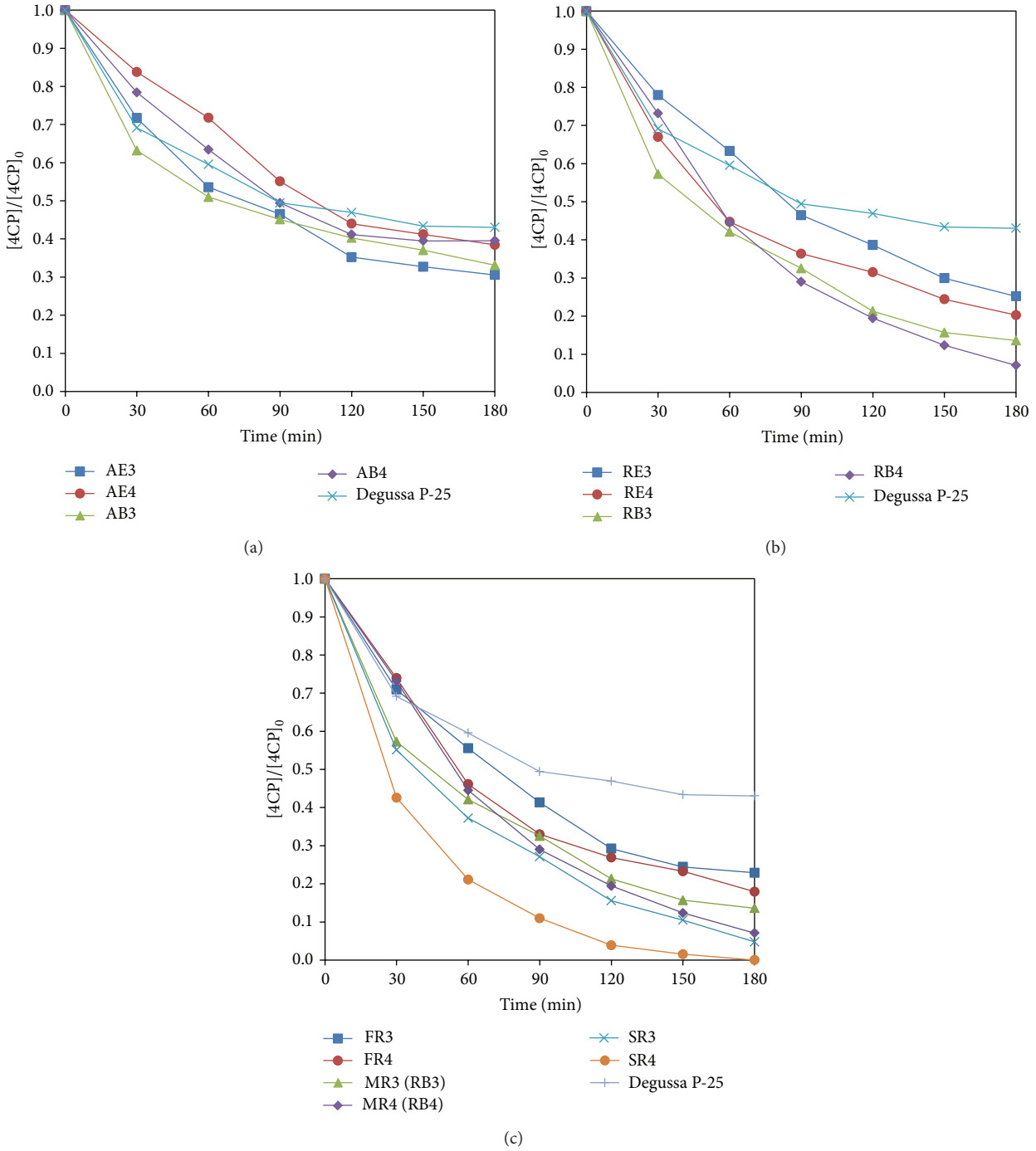

FIGURE 6: Photocatalytic degradation profiles of 4CP over the mesoporous titania samples synthesized with (a) room temperature, (b) rotary evaporator, (c) drying rate in rotary evaporator, and Degussa P-25.

which gives the following, after integration in the interval $[C, C_0]$:

$$\ln \frac{C_0}{C} = K_{ap} t. \quad (2)$$

Plotting $\ln(C_0/C)$ versus reaction time t yields a straight line, where the slope is the apparent rate constant. The half-life of the degraded organic compound can then be easily calculated. Figure 9 shows the lineal plot of 4CP photodegradation, which adjusts well to a pseudo-first-order kinetic behavior. Apparent constant K_{ap}, 4CP half-life, and the linearization coefficient r^2 are summarized in Table 4. 4CP half-life is as short as 25.6 min, with mesoporous titania sample SR4, and nearly 80% of initial 0.233 mmol L^{-1} is degraded in 60 minutes.

Table 5: COD values of the aqueous solution before and after photocatalytic tests, adsorption, and photolysis.

Sample	COD value (mg/L)	
	Initial (0 minutes)	Final (180 minutes)
SR4 (photocatalysis)	47	20
SR4 (adsorption)	47	47
Degussa P-25 (photocatalysis)	47	36
Photolysis	47	47

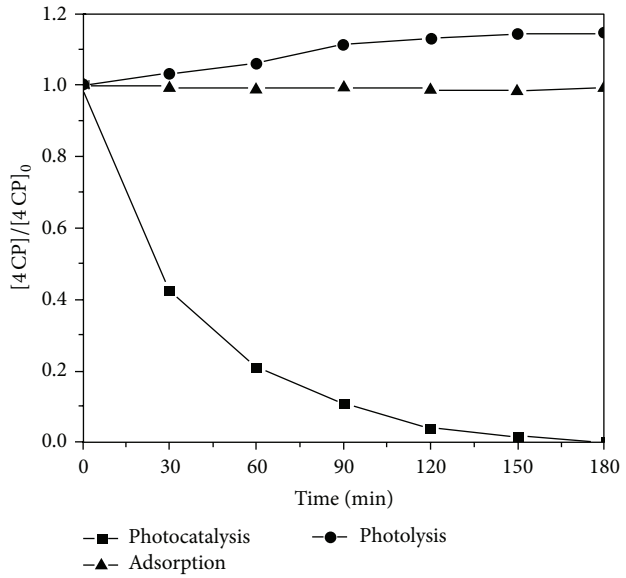

Figure 7: Effect of photocatalysis, adsorption, and photolysis on the removal of 4CP as a function of time using mesoporous titania sample SR4.

Table 5 shows the COD values to identify the presence of organic matter in the aqueous solution after photocatalytic tests. 4CP photodegradation using sample SR4 reduced the initial value of COD by 57%, whereas Degussa P-25 reduced the initial value of COD by 23% after the same time of exposure to UV irradiation. These results support the removal of 4CP by adsorption and photolysis shown in Figure 7, without reduction in initial values of COD. Therefore, it is demonstrated that the organic compound is mineralized. In specialized literature [34, 36], hydroquinone (HQ), benzoquinone (BQ), and 4-chlorocatechol (4CC) have been reported as the major aromatic intermediates, identified by HPLC, LC-MS, and GC-MS techniques. Although interesting, such characterization is beyond the scope of this paper.

4. Conclusions

Mesoporous nanocrystalline anatase was found to provide a faster degradation rate than Degussa P-25 as consequence of different surface morphological characteristics. Among the studied variables, different drying rate in rotary evaporator

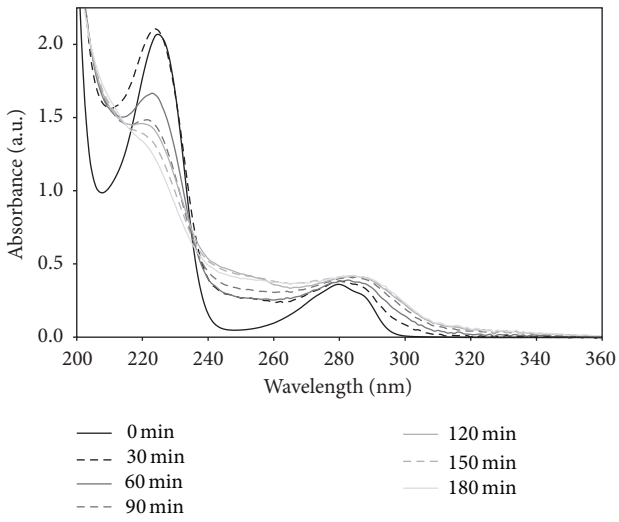

Figure 8: UV/Vis spectra of the 4CP degradation under photolysis.

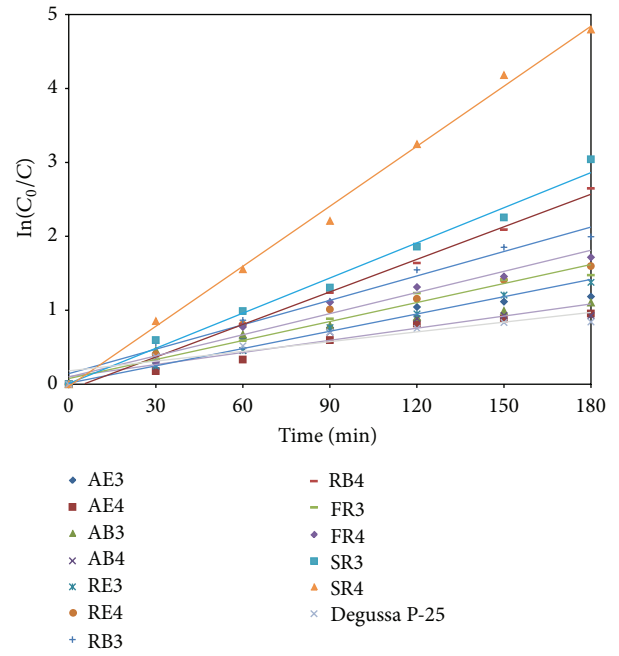

Figure 9: Pseudo-first-order kinetics degradation of 4CP, by the Langmuir-Hinshelwood model.

was determined to be the one that affects the increase in average pore diameter, and this affects both the percentage of photodegradation and the chemical oxygen demand (COD) value. The diffusion towards the active sites and the accessibility of the active sites for adsorption due to the presence of large pores are key parameters for the photocatalytic degradation of 4CP. The photodegradation process was found to be controlled by the Langmuir-Hinshelwood model. The mesoporous anatase degraded 100% 4CP, while Degussa P-25 degraded 57%. The enhanced photocatalytic activity of the

mesoporous titania samples when compared to Degussa P-25 was related to smaller crystallite size, presence of pure anatase phase, higher average pore diameter, and surface area. The reduction of 57% COD with mesoporous anatase compared with 23% Degussa P-25 shows that 4CP is mineralized.

Conflict of Interests

The authors declare that there is no conflict of interests regarding the publication of this paper.

Acknowledgments

The authors are grateful to PROMEP for financial support through Project 103.5/13/S257. Osmín Avilés-García thanks CONACYT for scholarship 290649 and CCIQS from UAEM for the granted support.

References

[1] R. W. Matthews, "Kinetics of photocatalytic oxidation of organic solutes over titanium dioxide," *Journal of Catalysis*, vol. 111, pp. 264–272, 1988.

[2] C. S. Turchi and D. F. Ollis, "Photocatalytic degradation of organic water contaminants: mechanisms involving hydroxyl radical attack," *Journal of Catalysis*, vol. 122, no. 1, pp. 178–192, 1990.

[3] D. W. Bahnemann, J. Cunningham, M. A. Fox, E. Pelizzetti, P. Pichat, and N. Serpone, "Photocatalytic treatment of waters," in *Aquatic Surface and Photochemistry*, R. G. Zepp, G. R. Helz, and D. G. Crosby, Eds., pp. 261–316, Lewis, Boca Raton, Fla, USA, 1994.

[4] M. R. Hoffmann, S. T. Martin, W. Choi, and D. W. Bahnemann, "Environmental applications of semiconductor photocatalysis," *Chemical Reviews*, vol. 95, no. 1, pp. 69–96, 1995.

[5] J.-M. Herrmann, "Heterogeneous photocatalysis: fundamentals and applications to the removal of various types of aqueous pollutants," *Catalysis Today*, vol. 53, no. 1, pp. 115–129, 1999.

[6] H. Yang, A. Kuperman, N. Coombs, S. Mamiche-Afara, and G. A. Ozin, "Synthesis of oriented films of mesoporous silica on mica," *Nature*, vol. 379, no. 6567, pp. 703–705, 1996.

[7] H. Yang, N. Coombs, I. Sokolov, and G. A. Ozin, "Free-standing and oriented mesoporous silica films grown at the air-water interface," *Nature*, vol. 381, no. 6583, pp. 589–592, 1996.

[8] Y. Lu, R. Ganguli, C. A. Drewien et al., "Continuous formation of supported cubic and hexagonal mesoporous films by sol-gel dip-coating," *Nature*, vol. 389, no. 6649, pp. 364–368, 1997.

[9] M. A. Carreon and V. V. Guliants, "Mesostructuring of metal oxides through EISA: fundamentals and applications," in *Ordered Porous Solids*, Chapter 16, pp. 413–439, 2009.

[10] G. J. D. A. A. Soler-Illia, A. Louis, and C. Sanchez, "Synthesis and characterization of mesostructured titania-based materials through evaporation-induced self-assembly," *Chemistry of Materials*, vol. 14, no. 2, pp. 750–759, 2002.

[11] K. De Witte, A. M. Busuioc, V. Meynen et al., "Influence of the synthesis parameters of TiO_2-SBA-15 materials on the adsorption and photodegradation of rhodamine-6G," *Microporous and Mesoporous Materials*, vol. 110, no. 1, pp. 100–110, 2008.

[12] M. A. Carreon, S. Y. Choi, M. Mamak, N. Chopra, and G. A. Ozin, "Pore architecture affects photocatalytic activity of periodic mesoporous nanocrystalline anatase thin films," *Journal of Materials Chemistry*, vol. 17, no. 1, pp. 82–89, 2007.

[13] M. L. Carreon, H. G. Carreon, J. Espino-Valencia, and M. A. Carreon, "Photocatalytic degradation of organic dyes by mesoporous nanocrystalline anatase," *Materials Chemistry and Physics*, vol. 125, no. 3, pp. 474–478, 2011.

[14] R. Andreozzi and R. Marotta, "Ozonation of p-chlorophenol in aqueous solution," *Journal of Hazardous Materials*, vol. 69, no. 3, pp. 303–317, 1999.

[15] C. H. Kuo and C. H. Huang, "Aqueous phase ozonation of chlorophenols," *Journal of Hazardous Materials*, vol. 41, no. 1, pp. 31–45, 1995.

[16] Y. Pi, L. Zhang, and J. Wang, "The formation and influence of hydrogen peroxide during ozonation of para-chlorophenol," *Journal of Hazardous Materials*, vol. 141, no. 3, pp. 707–712, 2007.

[17] M. L. Satuf, R. J. Brandi, A. E. Cassano, and O. M. Alfano, "Photocatalytic degradation of 4-chlorophenol: a kinetic study," *Applied Catalysis B: Environmental*, vol. 82, no. 1-2, pp. 37–49, 2008.

[18] J.-C. D'Oliveira, G. Al-Sayyed, and P. Pichat, "Photodegradation of 2- and 3-chlorophenol in TiO_2 aqueous suspensions," *Environmental Science and Technology*, vol. 24, no. 7, pp. 990–996, 1990.

[19] T. Pandiyan, O. M. Rivas, J. O. Martínez, G. B. Amezcua, and M. A. M. Carrillo, "Comparison of methods for the photochemical degradation of chlorophenols," *Journal of Photochemistry and Photobiology A: Chemistry*, vol. 146, pp. 149–155, 2002.

[20] J.-C. D'Oliveira, C. Minero, E. Pelizzetti, and P. Pichat, "Photodegradation of dichlorophenols and trichlorophenols in TiO_2 aqueous suspensions: kinetic effects of the positions of the Cl atoms and identification of the intermediates," *Journal of Photochemistry and Photobiology A: Chemistry*, vol. 72, no. 3, pp. 261–267, 1993.

[21] K. H. Wang, Y. H. Hsieh, M. Y. Chou, and C. Y. Chang, "Photocatalytic degradation of 2-chloro and 2-nitrophenol by titanium dioxide suspensions in aqueous solution," *Applied Catalysis B: Environmental*, vol. 21, pp. 1–8, 1999.

[22] Y.-C. Chan, J.-N. Chen, and M.-C. Lu, "Intermediate inhibition in the heterogeneous UV-catalysis using a TiO_2 suspension system," *Chemosphere*, vol. 45, no. 1, pp. 29–35, 2001.

[23] A. M. Peiró, J. A. Ayllón, J. Peral, and X. Doménech, "TIO_2-photocatalyzed degradation of phenol and *ortho*-substituted phenolic compounds," *Applied Catalysis B: Environmental*, vol. 30, pp. 359–373, 2001.

[24] U. Stafford, K. A. Gray, and P. V. Kamat, "Photocatalytic degradation of 4-chlorophenol: the effects of varying TiO_2 concentration and light wavelength," *Journal of Catalysis*, vol. 167, no. 1, pp. 25–32, 1997.

[25] U. Stafford, K. A. Gray, and P. V. Kamat, "Radiolytic and TiO_2-assisted photocatalytic degradation of 4-chlorophenol. A comparative study," *Journal of Physical Chemistry*, vol. 98, no. 25, pp. 6343–6351, 1994.

[26] A. Mills and J. Wang, "Photomineralisation of 4-chlorophenol sensitised by TiO_2 thin films," *Journal of Photochemistry and Photobiology A: Chemistry*, vol. 118, pp. 53–63, 1998.

[27] X. Li, J. W. Cubbage, T. A. Tetzlaff, and W. S. Jenks, "Photocatalytic degradation of 4-chlorophenol. 1. The hydroquinone pathway," *Journal of Organic Chemistry*, vol. 64, no. 23, pp. 8509–8524, 1999.

[28] X. Li, J. W. Cubbage, and W. S. Jenks, "Photocatalytic degradation of 4-chlorophenol. 2. The 4-chlorocatechol pathway,"

Journal of Organic Chemistry, vol. 64, no. 23, pp. 8525–8536, 1999.

[29] E. M. Campo, J. S. Valente, T. Pavón, R. Romero, Á. Mantilla, and R. Natividad, "4-chlorophenol oxidation photocatalyzed by a calcined Mg–Al–Zn layered double hydroxide in a co-current downflow bubble column," *Industrial & Engineering Chemistry Research*, vol. 50, pp. 11544–11552, 2011.

[30] H. Al-Ekabi, N. Serpone, E. Pelizzetti, C. Minero, M. A. Fox, and R. B. Draper, "Kinetic studies in heterogeneous photocatalysis. 2. TiO_2-mediated degradation of 4-chlorophenol alone and in a three-component mixture of 4-chlorophenol, 2,4-dichlorophenol, and 2,4,5-trichlorophenol in air-equilibrated aqueous media," *Langmuir*, vol. 5, no. 1, pp. 250–255, 1989.

[31] R. W. Matthews, "Purification of water with near-U.V. illuminated suspensions of titanium dioxide," *Water Research*, vol. 24, no. 5, pp. 653–660, 1990.

[32] G. Al-Sayyed, J. C. D'Oliveira, and P. Pichat, "Semiconductor-sensitized photodegradation of 4-chlorophenol in water," *Journal of Photochemistry and Photobiology A: Chemistry*, vol. 58, pp. 99–114, 1991.

[33] A. Mills, S. Morris, and R. Davies, "Photomineralisation of 4-chlorophenol sensitised by titanium dioxide: a study of the intermediates," *Journal of Photochemistry and Photobiology A: Chemistry*, vol. 70, pp. 183–191, 1993.

[34] A. Mills and S. Morris, "Photomineralization of 4-chlorophenol sensitized by titanium dioxide: a study of the initial kinetics of carbon dioxide photogeneration," *Journal of Photochemistry and Photobiology A: Chemistry*, vol. 71, pp. 75–83, 1993.

[35] J. Theurich, M. Lindner, and D. W. Bahnemann, "Photocatalytic degradation of 4-chlorophenol in aerated aqueous titanium dioxide suspensions: a kinetic and mechanistic study," *Langmuir*, vol. 12, no. 26, pp. 6368–6376, 1996.

[36] M. Hügül, I. Boz, and R. Apak, "Photocatalytic decomposition of 4-chlorophenol over oxide catalysts," *Journal of Hazardous Materials*, vol. 64, no. 3, pp. 313–322, 1999.

[37] M. Fröba, O. Muth, and A. Reller, "Mesostructured TiO_2: ligand-stabilized synthesis and characterization," *Solid State Ionics*, vol. 101–103, no. 1, pp. 249–253, 1997.

[38] S. Cabrera, J. El Haskouri, A. Beltrán-Porter, D. Beltrán-Porter, M. D. Marcos, and P. Amorós, "Enhanced surface area in thermally stable pure mesoporous TiO_2," *Solid State Sciences*, vol. 2, pp. 513–518, 2000.

[39] A. Gibaud, D. Grosso, B. Smarsly et al., "Evaporation-controlled self-assembly of silica surfactant mesophases," *Journal of Physical Chemistry B*, vol. 107, no. 25, pp. 6114–6118, 2003.

[40] T. Hongo and A. Yamazaki, "Thermal influence on the structure and photocatalytic activity of mesoporous titania consisting of TiO_2(B)," *Microporous and Mesoporous Materials*, vol. 142, no. 1, pp. 316–321, 2011.

[41] E. L. Crepaldi, G. J. D. A. A. Soler-Illia, D. Grosso, F. Cagnol, F. Ribot, and C. Sanchez, "Controlled formation of highly organized mesoporous titania thin films: from mesostructured hybrids to mesoporous nanoanatase TiO_2," *Journal of the American Chemical Society*, vol. 125, no. 32, pp. 9770–9786, 2003.

[42] K. S. W. Sing, D. H. Everett, R. A. W. Haul et al., "Reporting physisorption data for gas/solid systems with special reference to the determination of surface area and porosity (Recommendations 1984)," *Pure and Applied Chemistry*, vol. 57, pp. 603–619, 1985.

[43] T. Ohno, K. Sarukawa, K. Tokieda, and M. Matsumura, "Morphology of a TiO_2 photocatalyst (Degussa, P-25) consisting of anatase and rutile crystalline phases," *Journal of Catalysis*, vol. 203, no. 1, pp. 82–86, 2001.

[44] A. Katti, S. R. Venna, and M. A. Carreon, "Self-assembly hydrothermal assisted synthesis of mesoporous anatase in the presence of ethylene glycol," *Catalysis Communications*, vol. 10, no. 15, pp. 2036–2040, 2009.

[45] A. Mills and S. LeHunte, "An overview of semiconductor photocatalysis," *Journal of Photochemistry and Photobiology A: Chemistry*, vol. 108, pp. 1–35, 1997.

[46] Y. Sakatani, D. Grosso, L. Nicole, C. Boissiere, G. J. D. A. A. Soller-Illia, and C. Sanchez, "Optimised photocatalytic activity of grid-like mesoporous TiO_2 films: effect of crystallinity, pore size distribution, and pore accessibility," *Journal of Materials Chemistry*, vol. 16, pp. 77–82, 2006.

[47] K. De Witte, S. Ribbens, V. Meynen et al., "Photocatalytic study of P25 and mesoporous titania in aqueous and gaseous environment," *Catalysis Communications*, vol. 9, no. 8, pp. 1787–1792, 2008.

[48] E. Beyers, P. Cool, and E. F. Vansant, "Stabilisation of mesoporous TiO_2 by different bases influencing the photocatalytic activity," *Microporous and Mesoporous Materials*, vol. 99, no. 1-2, pp. 112–117, 2007.

[49] J. W. Moon, C. Y. Yun, and K. W. Chung, "Photocatalytic activation of TiO_2 under visible light using Acid Red 44," *Catalysis Today*, vol. 87, pp. 77–86, 2003.

[50] E. P. Reddy, B. Sun, and P. G. Smiriniotis, "Transition metal modified TiO_2-loaded MCM-41 catalysts for visible- and UV-light driven photodegradation of aqueous organic pollutants," *The Journal of Physical Chemistry B*, vol. 108, pp. 17198–17205, 2004.

[51] J. S. Valente, F. Tzompantzi, J. Prince, J. G. H. Cortez, and R. Gomez, "Adsorption and photocatalytic degradation of phenol and 2,4 dichlorophenoxiacetic acid by Mg-Zn-Al layered double hydroxides," *Applied Catalysis B: Environmental*, vol. 90, no. 3-4, pp. 330–338, 2009.

[52] J. S. Valente, F. Tzompantzi, and J. Prince, "Highly efficient photocatalytic elimination of phenol and chlorinated phenols by CeO_2/MgAl layered double hydroxides," *Applied Catalysis B: Environmental*, vol. 102, no. 1-2, pp. 276–285, 2011.

[53] G. Sivalingam, M. H. Priya, and G. Madras, "Kinetics of the photodegradation of substituted phenols by solution combustion synthesized TiO_2," *Applied Catalysis B: Environmental*, vol. 51, no. 1, pp. 67–76, 2004.